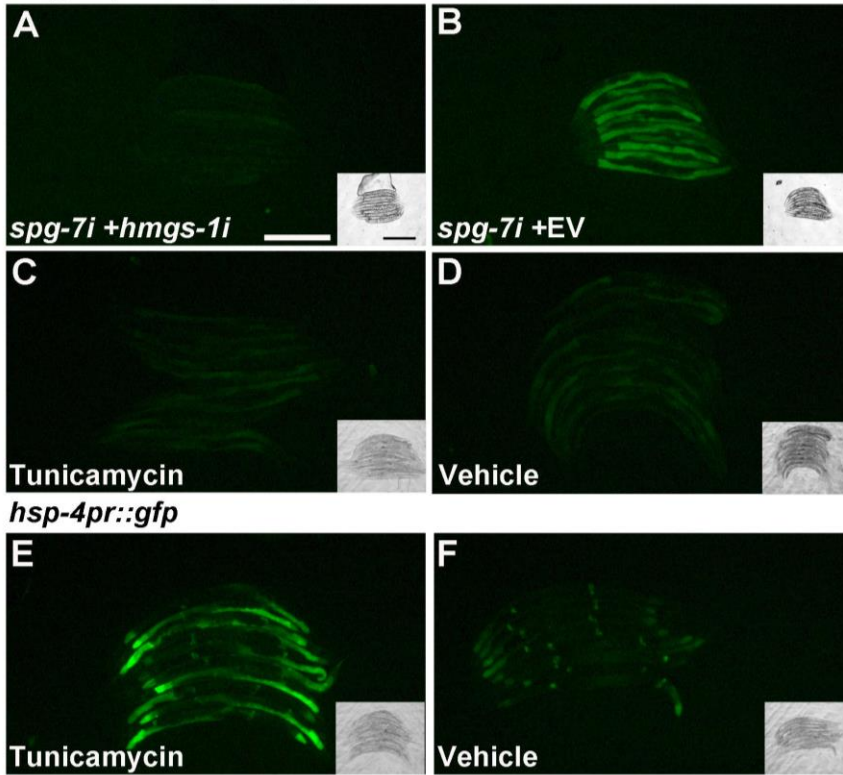


## Supplemental materials

*hmgs-1pr::hmgs-1::gfp*



**Figure S1. The UPR<sup>er</sup> does not upregulate HMGS-1**

A) *hmgs-1* double strand RNA (dsRNA) abolishes the upregulation of HMGS-1::GFP by *spg-7* RNAi. This effect of *hmgs-1* RNAi demonstrates the specificity of both the *hmgs-1pr::hmgs-1::gfp* construct (hereafter HMGS-1::GFP) and the *hmgs-1* RNAi clone. B) *spg-7* dsRNA upregulates HMGS-1::GFP even when diluted in half with an empty vector control. This upregulation shows that the lack of HMGS-1::GFP upregulation in panel A did not stem from diluting the effect of *spg-7* RNAi. C) UPR<sup>er</sup>, induced by tunicamycin (5µg/ml), does not upregulate HMGS-1::GFP. D) HMGS-1::GFP worms in 0.1% DMSO (vehicle for the tunicamycin treatment). E) 5µg/ml Tunicamycin induces UPR<sup>er</sup> in comparison to 0.1% DMSO control (F). Hereafter, all worms were analyzed at the chronological age of day one or two of adulthood. In each experiment, control and experimental worms were synchronized and analyzed at the exact same chronological

age. “i” represents RNAi, e.g. *spg-7* RNAi is *spg-7i*; EV stands for an empty vector control. Scale bars represent 250µm and 500µm (inserts).

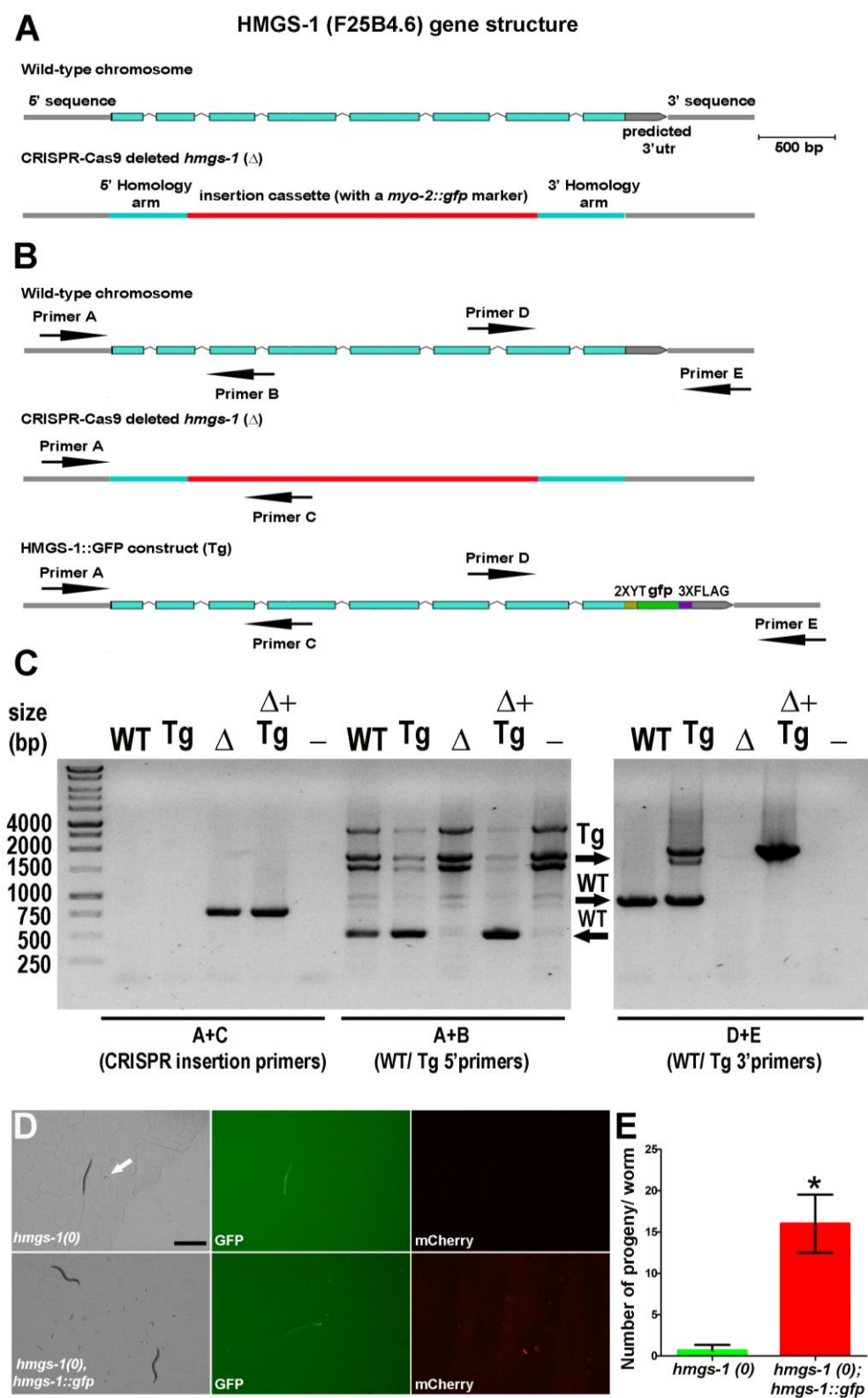


## Figure S2. HMGS-1::GFP rescues the phenotypes of *hmgs-1* loss

A) The structure of the *C. elegans hmgs-1* (F25B4.6) gene and the CRISPR-Cas9 integration cassette. B) Locations of the primers used to distinguish between the wild-type chromosome, the rearranged *hmgs-1* locus, and the HMGS-1::GFP construct. C) PCR analysis of the different genetic backgrounds. D) The livelihood and progeny of worms homozygous for the *hmgs-1* deletion and worms from the same genetic background that express the HMGS-1::GFP construct. Both types of worms were grown on plates with 20mM mevalonate and were transferred to plates without mevalonate at larval stage four and imaged after 96 hours. A white arrow marks two dead embryos (the only embryos on plates with *hmgs-1* knockout worms). The panels of “D” are of the same worms in different time frames. E) The HMGS-1::GFP construct rescues the lethality and sterility of the *hmgs-1* loss of function allele. Number of progeny 96 hours after the L4 stage of *hmgs-1* (0) worms, with or without the HMGS-1::GFP construct. n(number of worms tested for the number of progeny)= 3 for each condition. Graph bars represent standard errors. “\*” $p \leq 0.05$  using an unpaired, two-tailed Student’s T-test. The scale bar in panel “D” represents 1mm.

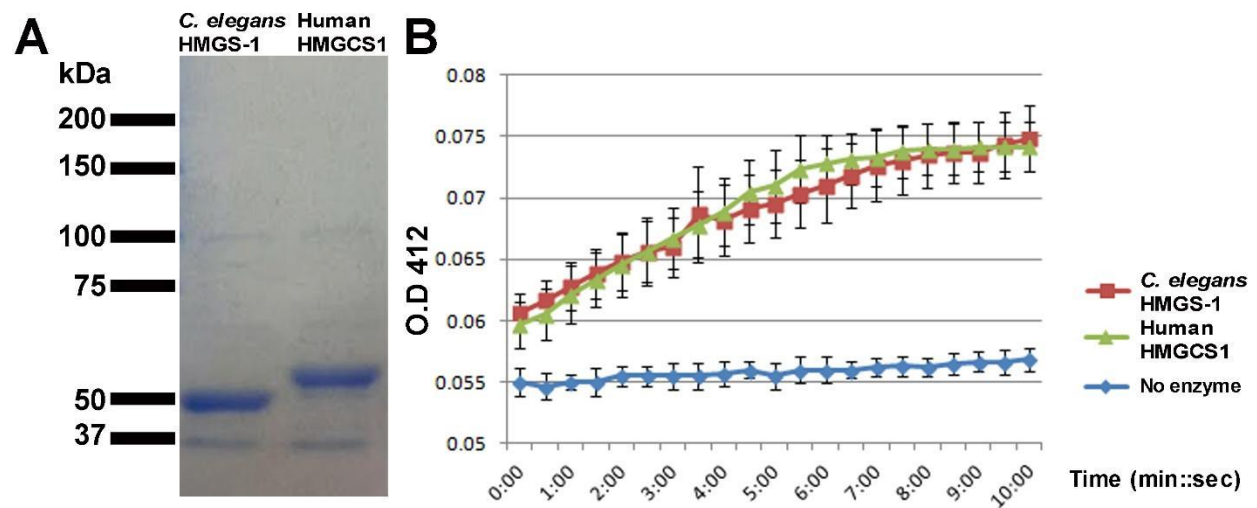


**Figure S3. *In vitro*, the *C. elegans* HMGS-1 enzyme catalyzes the first dedicated step of the mevalonate pathway**

A) *C. elegans* HMGS-1 and Human HMGCS1 proteins were cloned, expressed in bacteria, and purified. Sizes of HMGS-1 and HMGCS1 proteins are in agreement with the size predicted by their amino acid sequences with 6Xhis tags, i.e. 51.4 and 57.3 kDa, respectively. The molecular weights of the proteins were calculated with the ExPASy Compute pI/Mw tool ([http://web.expasy.org/compute\\_pi/](http://web.expasy.org/compute_pi/)). B) A biochemical assay for the conversion of Acetyl-CoA and Acetoacetyl-CoA to HMG-CoA. The accumulation of products as a function of time is depicted. Bars represent Standard Errors across three repetitions. The *in-vitro* assay reveals the functional orthology of HMGCS1 and HMGS-1 in converting Acetyl-CoA and Acetoacetyl-CoA to HMG-CoA. Enzyme activities in the linear region of the graphs (between 00:30 and 03:30) are 0.466 units  $\pm$  0.25 for HMGS-1 and 0.488 units  $\pm$  0.054 for HMGCS1. Definition of a unit= 1  $\mu$ M substrate converted to product per minute per 1  $\mu$ g of a purified enzyme. Technical details about the *in vitro* assay appear in the supplemental methods section.

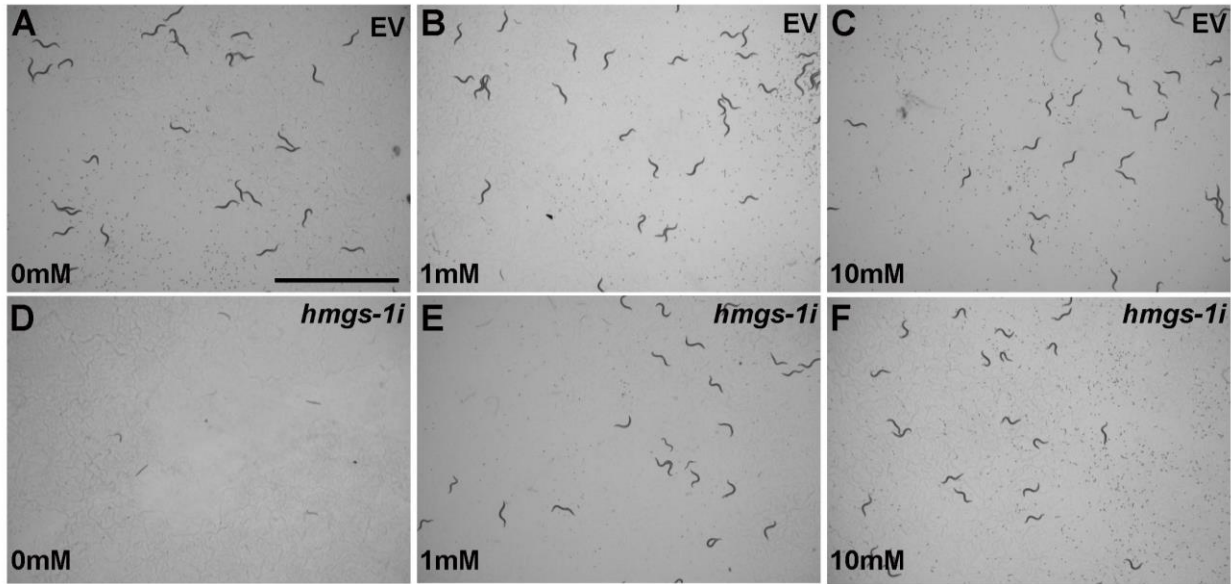


**Figure S4. Mevalonate rescues the severe phenotypes of *hmgs-1* knockdown**

A-C) N2 worms grown on control RNAi (an empty vector), with different concentrations of mevalonate. D-F) N2 worms grown on *hmgs-1* RNAi with different concentrations of mevalonate. The scale bar represents 5mm.

*isp-1 (0); hmgs-1<sup>pr::hmgs-1::gfp</sup>*

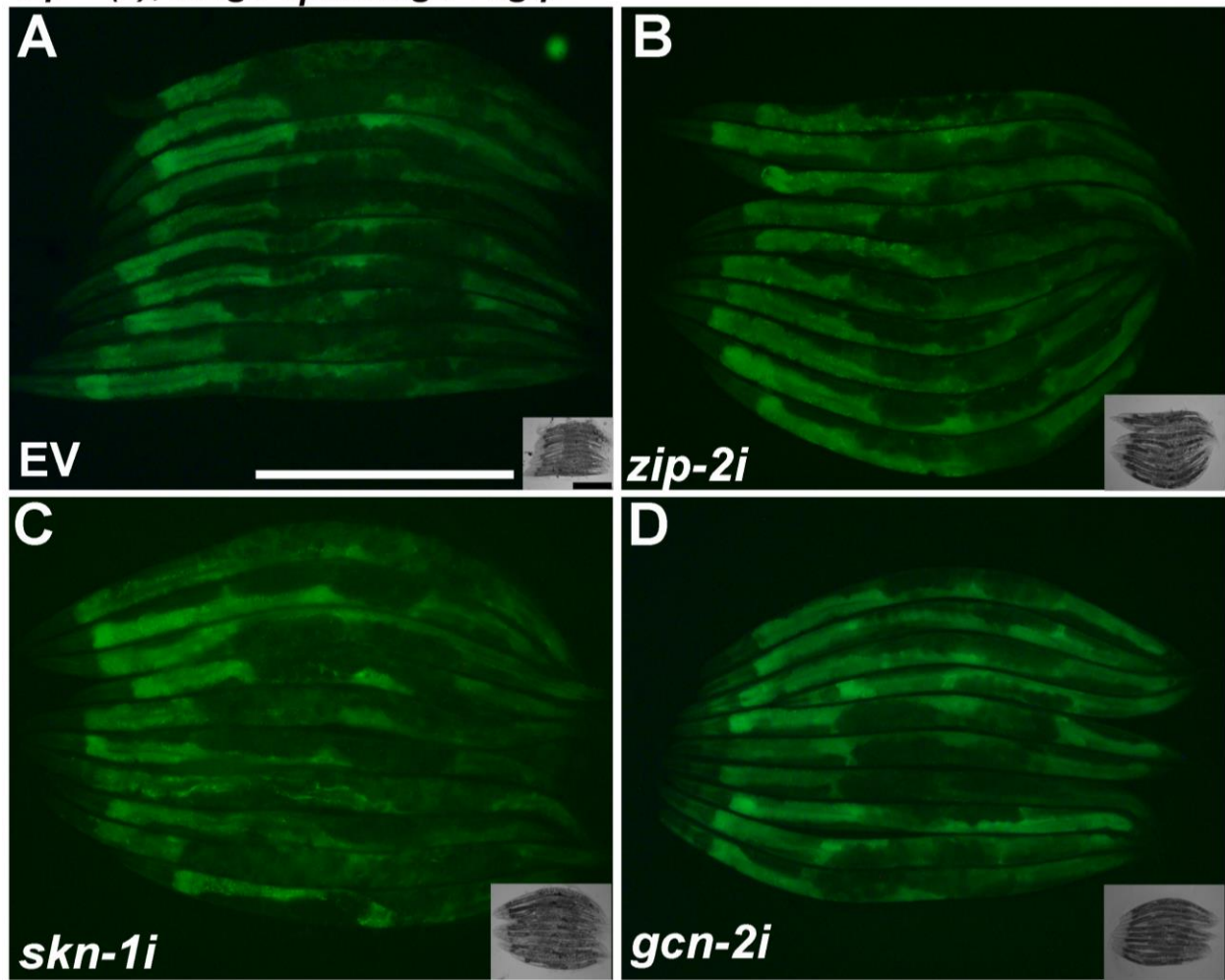


**Figure S5. Genes that have a primary role in the mitochondrial stress response but do not alter the levels of HMGS-1::GFP during mitochondrial stress**

A) HMGS-1::GFP in *isp-1(qm150)* mutant worms fed an empty vector control. In the same genetic background, *zip-2* RNAi (B), *skn-1* RNAi (C) and *gcn-2* RNAi (D) do not alter the levels of the HMGS-1::GFP signal. The scale bars represent 500 μm.

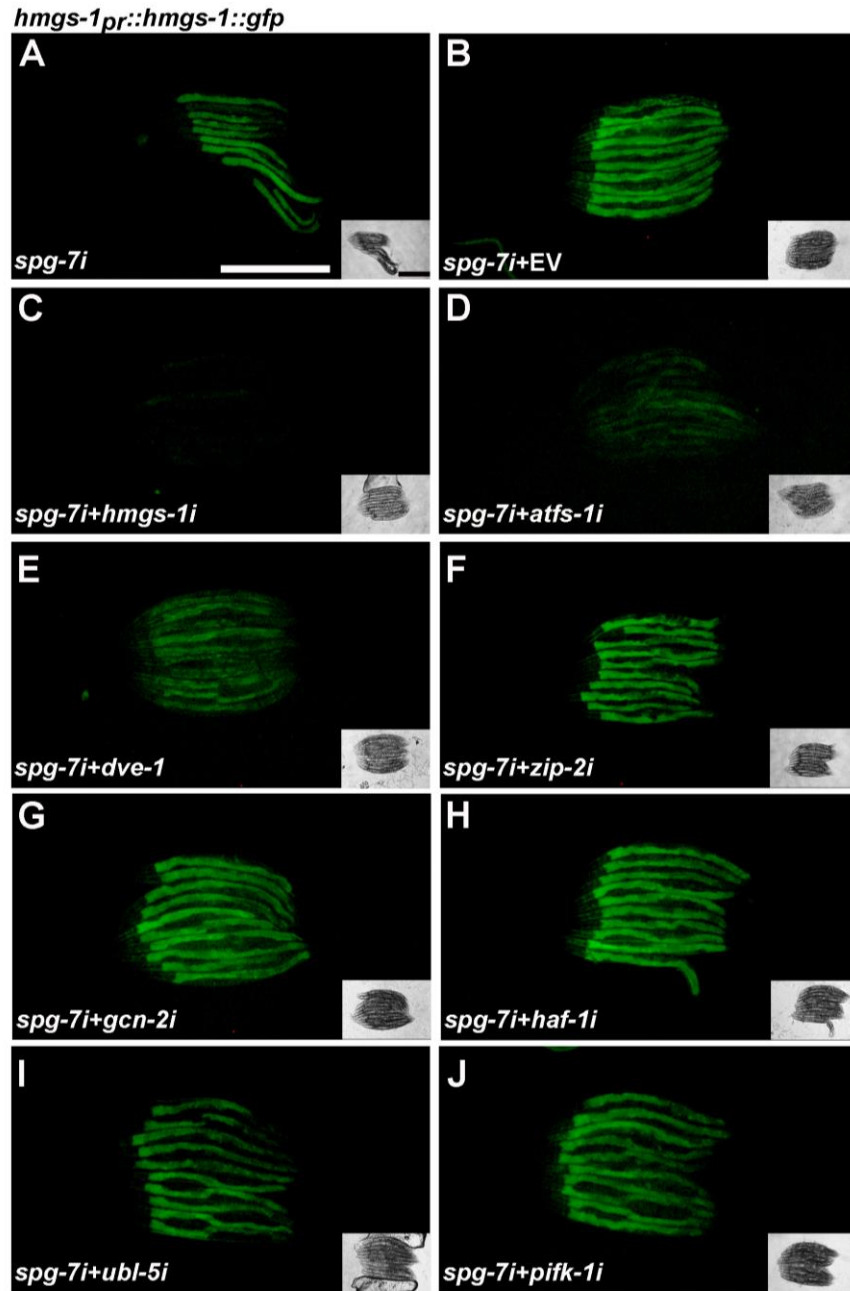


**Figure S6. HMGS-1 upregulation is dependent upon *atfs-1* and *dve-1***

A, B) As in the case of the *isp-1(qm150)*-induced UPR<sup>mt</sup> (Fig. 2), the UPR<sup>mt</sup> induced by *spg-7* RNAi upregulates HMGS-1::GFP. C- E) *hmgs-1*, *atfs-1*, and *dve-1* RNAis impede this upregulation. Consistent with Fig. S5, in the *spg-7* RNAi background, *zip-2* (F), and *gcn-2* (G) RNAis do not change the levels of HMGS-1 upregulation in mitochondrial

stress. Other genes that were suggested to play a role in the UPR<sup>mt</sup>, e.g. *haf-1* (H) *ubl-5* (I) and *pifk-1* (J), did not alter the level of HMGS-1::GFP protein upon UPR<sup>mt</sup> induction. Scale bars represent 500µm and 200µm (inserts).

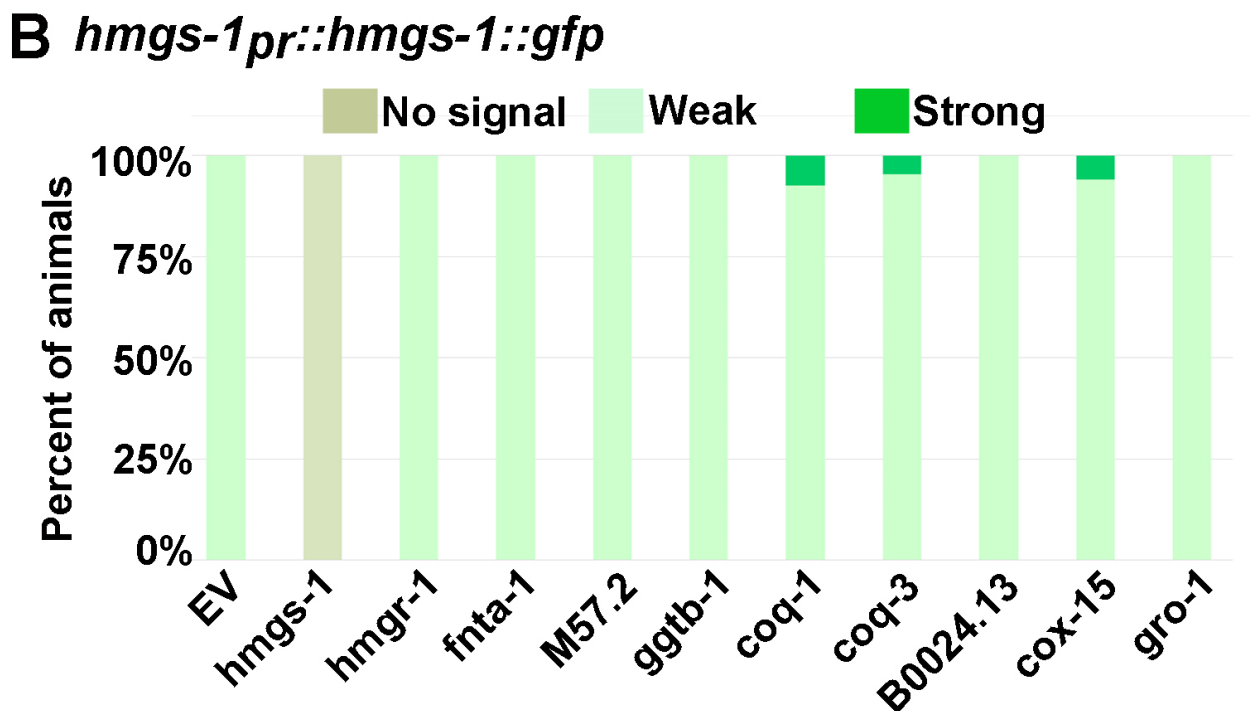
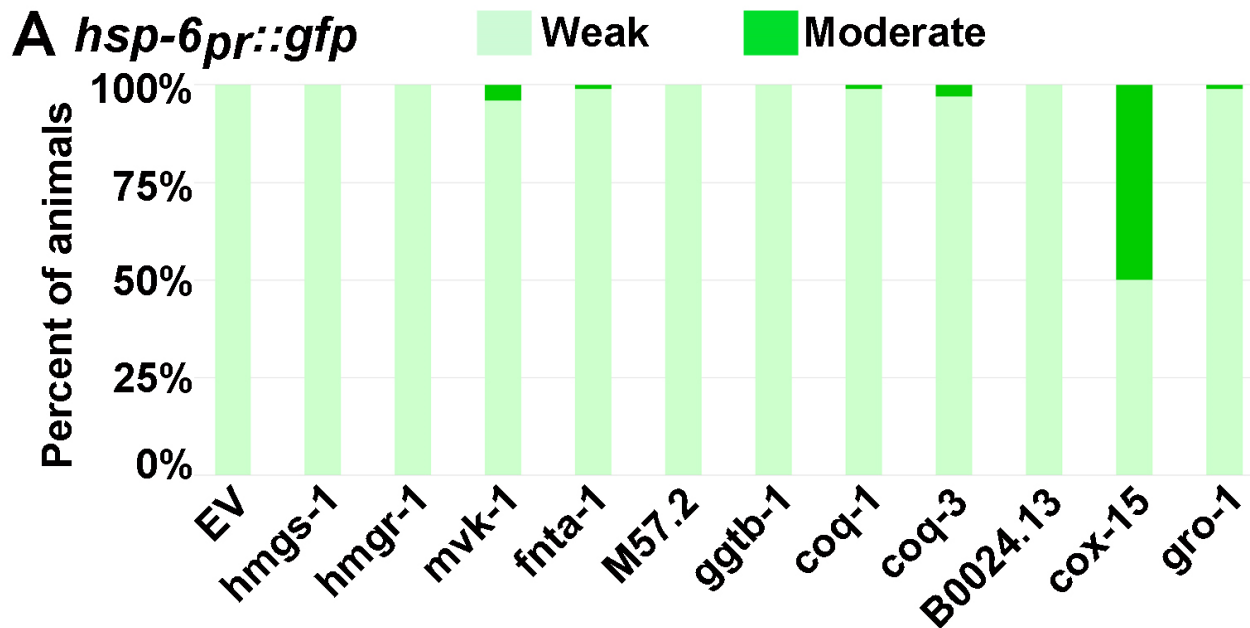


### Figure S7. Knockdown of hemeA synthesis induces the UPR<sup>mt</sup>

The effect of knockdown of different mevalonate pathway enzymes on UPR<sup>mt</sup> activation and HMGS-1::GFP expression. A) Knockdown of *cox-15* results UPR<sup>mt</sup> activation monitored by the *hsp-6<sub>pr</sub>::gfp* reporter. B) Knockdown of *coq-1*, *coq-3*, and *cox-15* that are responsible for the synthesis of the mitochondrial electron carriers ubiquinone and HemeA leads to HMGS-1::GFP upregulation. For each dsRNA tested, the results are presented as the percent of worms with a given signal from the total number of worms scored. n(number of worms examined in each RNAi treatment)= 100 for the *hsp-6<sub>pr</sub>::gfp* strain and 60-95 for the HMGS-1::GFP strain.

#### *hsp-6<sub>pr</sub>::gfp*

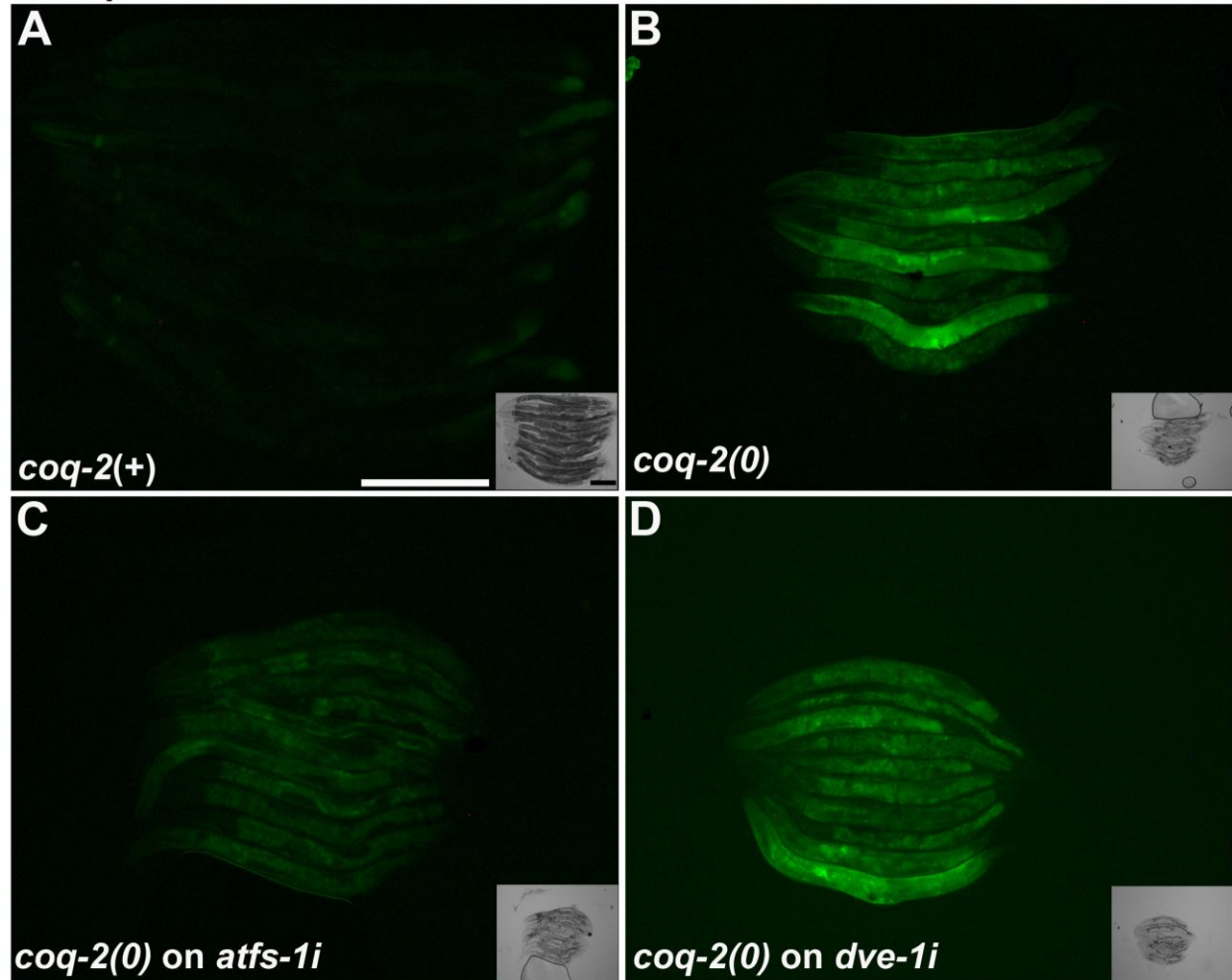


**Figure S8. Loss of *coq-2* activity results in UPR<sup>mt</sup> activation**

A) *hsp-6<sub>pr</sub>::gfp* in *coq-2*(+) worms. B) Loss of *coq-2* results in the activation of the UPR<sup>mt</sup> response. C) *hsp-6<sub>pr</sub>::gfp* upregulation is dependent upon *atfs-1* but not upon *dve-1* (D). Panel “A” is taken from Fig. 3E. Scale bars represent 250µm.

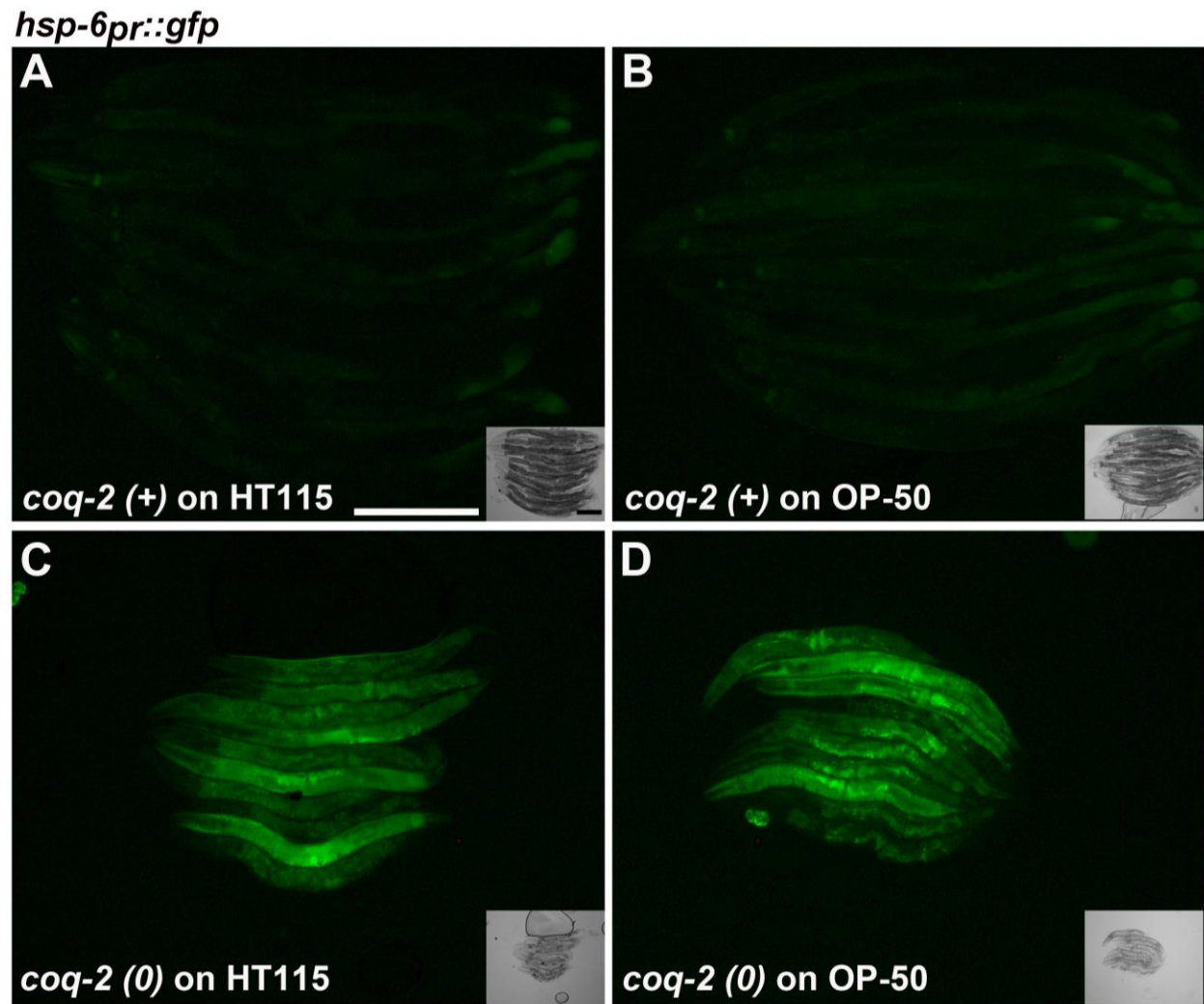


**Figure S9. The induction of the UPR<sup>mt</sup> by *coq-2* loss is not affected by the type of bacterial food source**

We examined whether the diet of HT115 bacteria, used in RNAi experiments, affects the levels of the UPR<sup>mt</sup>. A) *hsp-6<sub>pr</sub>::gfp* levels in *coq-2*(+) worms grown on HT115

bacteria. B) The standard bacterial food of *C. elegans*, OP-50, does not alter *hsp-6pr::gfp* expression pattern. C) In the background of *coq-2* loss of function mutation, *hsp-6pr::gfp* is upregulated in worms fed either HT115 bacteria or OP-50 bacteria (D). Panel “A” is taken from Fig. 3E and panel “C” from Fig. S8B. Scale bars represent 250µm.

***hmgs-1pr::hmgs-1::gfp***

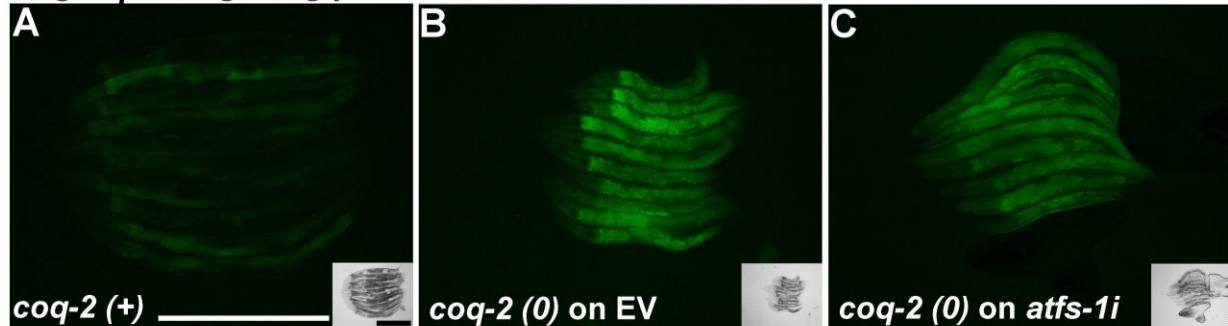


**Figure S10. Loss of ubiquinone synthesis leads to the upregulation of HMGS-1**

A) *HMGS-1::GFP* in wild-type worms fed an empty vector control. B) *HMGS-1::GFP* upregulation in a *coq-2* mutant background. C) *HMGS-1::GFP* upregulation in a *coq-2* mutant background is mildly affected by *atfs-1* RNAi. Scale bars represent 500µm.

***hsp-4pr::gfp***

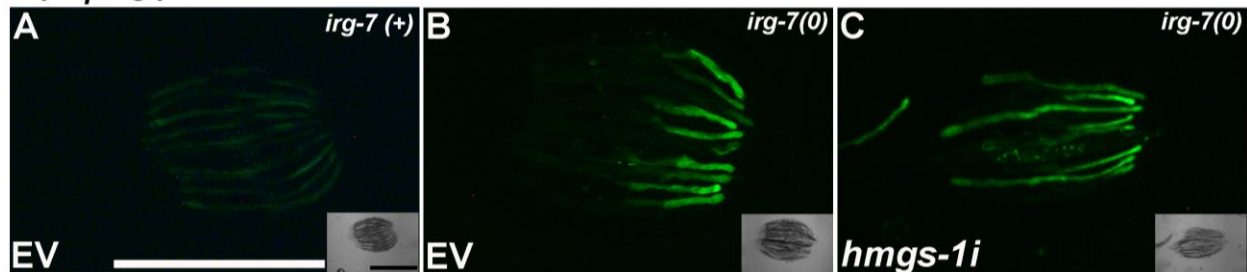


**Figure S11. *hmgs-1* knockdown does not block the UPR<sup>er</sup>**

A) The reporter for UPR<sup>er</sup>, *hsp-4pr::gfp*, in worms fed with bacteria transfected with an empty vector RNAi control. B) A mutation in the *irg-7* gene (*zc6*) induces a constitutive ER stress response, as monitored by the upregulation of the *hsp-4pr::gfp* reporter. C) Knockdown of *hmgs-1* by RNAi does not change the levels of UPR<sup>er</sup> activation. The scale bars represent 1mm.

*isp-1(0); hsp-6pr::gfp*

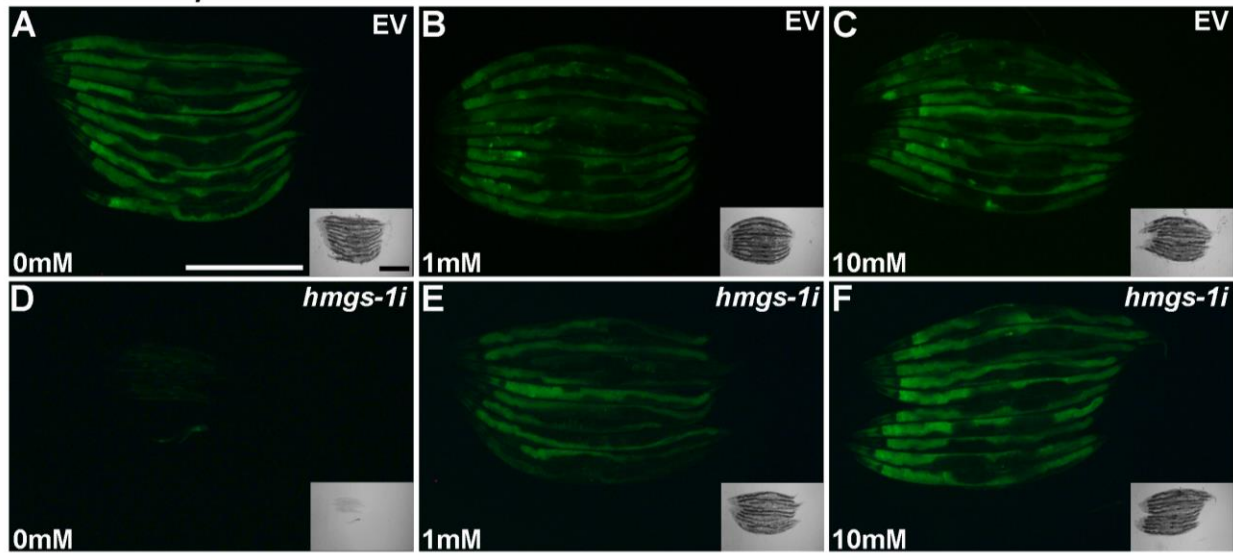


**Figure S12. Mevalonate rescues the inhibitory effect of *hmgs-1* RNAi**

A-C) Different concentrations of mevalonate do not significantly alter the level of UPR<sup>mt</sup> activation in EV control. D-F) In the presence of *hmgs-1* RNAi, an increase in the concentration of mevalonate unleashes the UPR<sup>mt</sup> response. Scales bars represent 500µm.

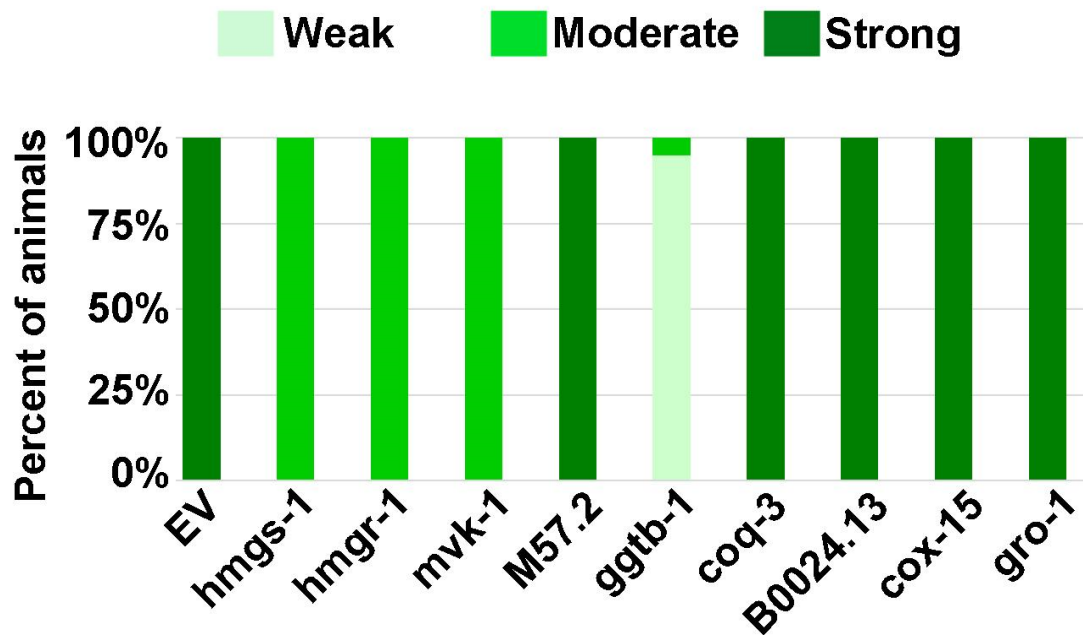


**Figure S13. Inhibition of either the main branch or the geranylgeranylation sub-branch of the mevalonate pathway block the UPR<sup>mt</sup>**

A targeted screen for the involvement of enzymes of the mevalonate pathway in the UPR<sup>mt</sup> response was conducted using the *isp-1(qm150); hsp-6<sub>pr</sub>::gfp* strain. Knockdown of enzymes in the main branch or in the geranylgeranylation sub-branch reduced the level of the *hsp-6<sub>pr</sub>::gfp* signal. Knockdown of proteins that play a role in the metabolism of other sub-branches does not change the level of *hsp-6<sub>pr</sub>::gfp* in comparison to the empty vector control. The screen was performed by the analysis of live intact worms under a fluorescence-dissecting microscope, which enabled qualitative sorting of the worms into the three different categories. n(number of worms examined in each RNAi treatment) =30.

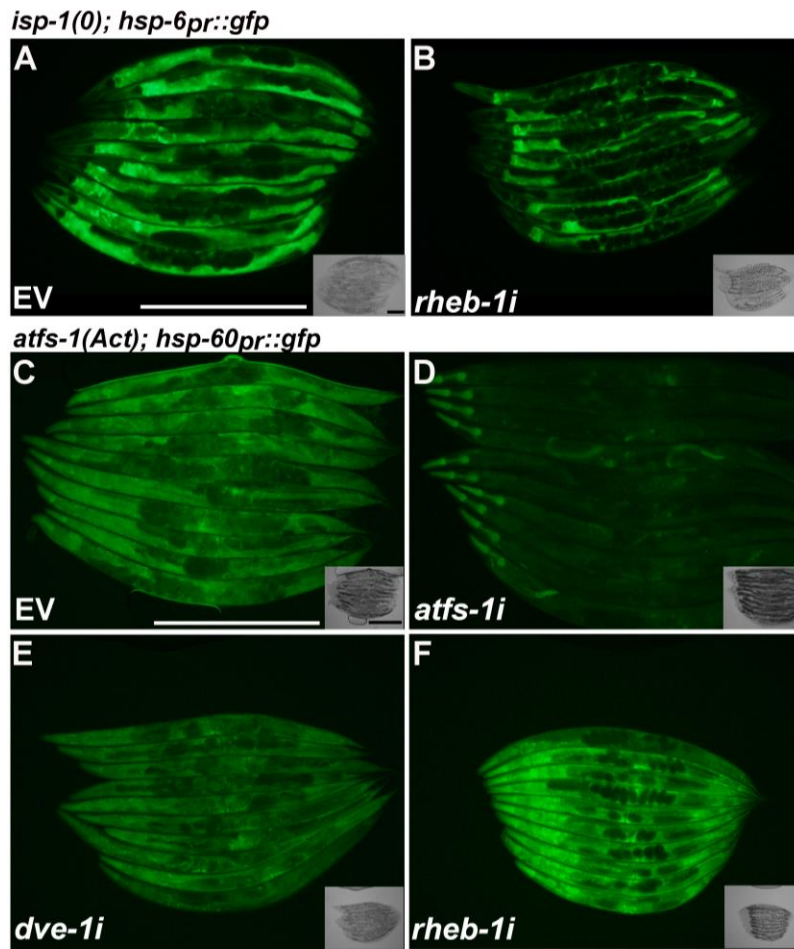


### Figure S14. RHEB-1 acts upstream or in parallel to ATFS-1

A) The UPR<sup>mt</sup> in *isp-1(qm150); hsp-6<sub>pr</sub>::gfp* worms. B) Knockdown of *rheb-1* decreases the level of UPR<sup>mt</sup> activation. C) Constitutively-activated ATFS-1 induces the UPR<sup>mt</sup> in unstressed worms as monitored by the *hsp-60<sub>pr</sub>::gfp* reporter. D) *atfs-1* RNAi abolishes the induction of *hsp-60<sub>pr</sub>::gfp* in most tissues of the worm. E) *dve-1* and F) *rheb-1* RNAis do not suppress the induction of the UPR<sup>mt</sup> by the activated ATFS-1 protein. Surprisingly, the *hsp-60<sub>pr</sub>::gfp* signal in the *rheb-1* RNAi background appears stronger than in the empty vector control. This difference raises the possibility that RHEB-1 functions as an inhibitor of ATFS-1-dependent transcription. This intriguing crosstalk between ATFS-1 and RHEB-1 requires future investigation. Scale bars represent 500µm and 50µm in inserts (A-B) and 500µm (C-F).

# Overlay of DIC and GFP

# GFP

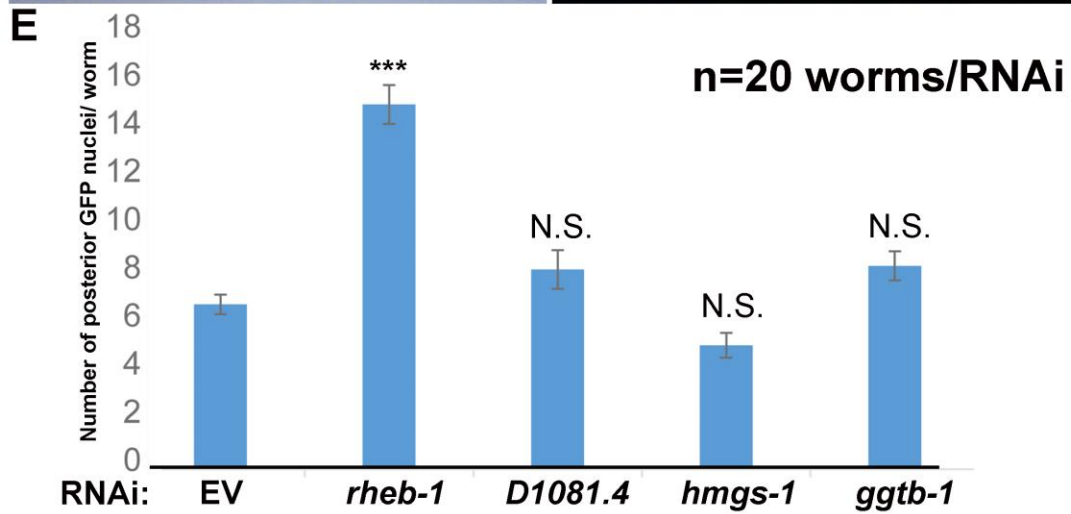
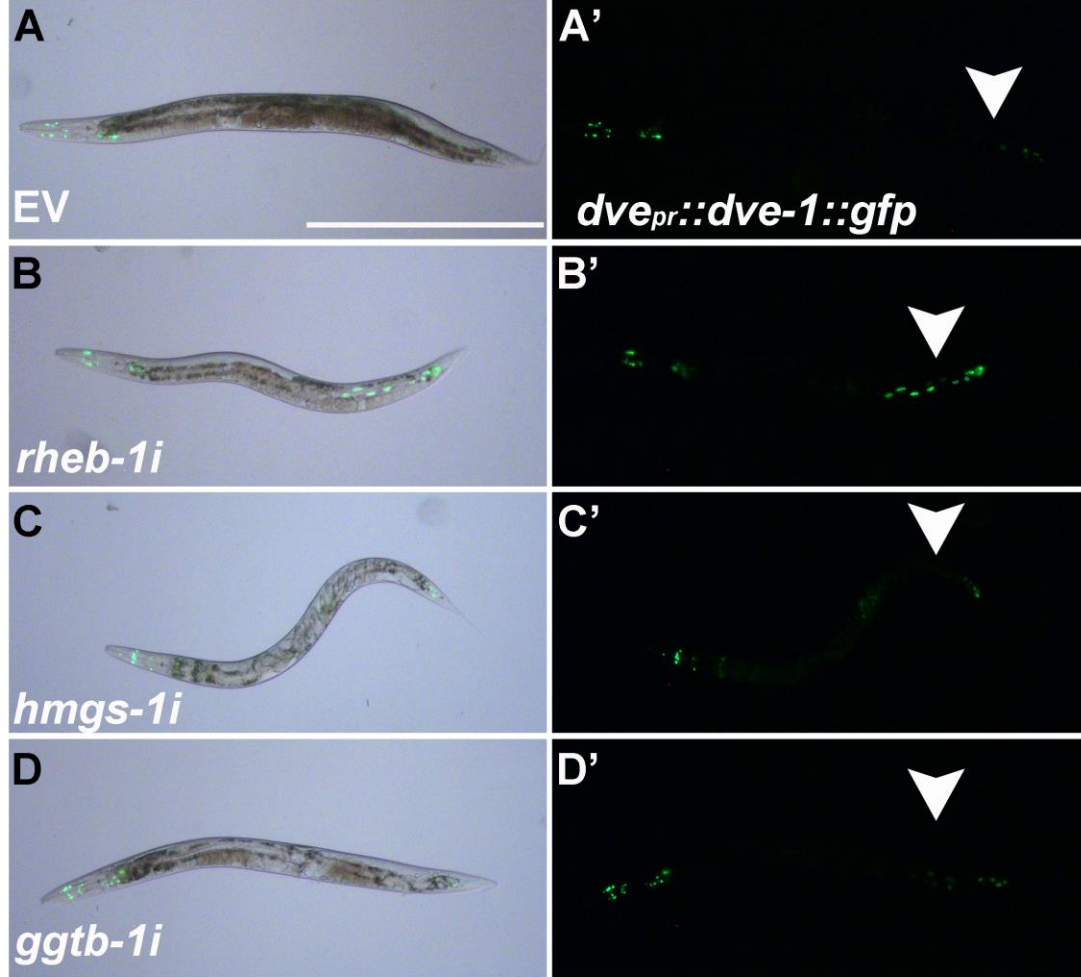


## Figure S15. Compromised mevalonate pathway metabolism does not to impede RHEB-1 activation

A) In a control RNAi (EV), DVE-1::GFP accumulates in a few nuclei at the head; and at the posterior side (arrowhead) of the worms. B) *rheb-1* knockdown results in an increased number of DVE-1::GFP-expressing nuclei at the posterior side of the animal. C) Knockdowns of the main branch and the geranylgeranylation sub-branch (D) of the mevalonate pathway do not alter the number of DVE-1::GFP-expressing nuclei in comparison to the control worms. E) A graph showing the number of nuclei per worm (n= 20 worms) per condition. D1081.4 is RHEB-1's closest paralog (GALLEGOS *et al.* 2012). Statistical significance was calculated by one-way ANOVA ( $F= 27.833$ ,  $\text{sig}<0.05$ ) after verifying normality by the Spiro-Wilck test and the analysis of variance by the Scheffe post-hoc test. “\*\*\*\*” $P\leq 0.001$ . The Scale bar represents 500 $\mu\text{m}$ .

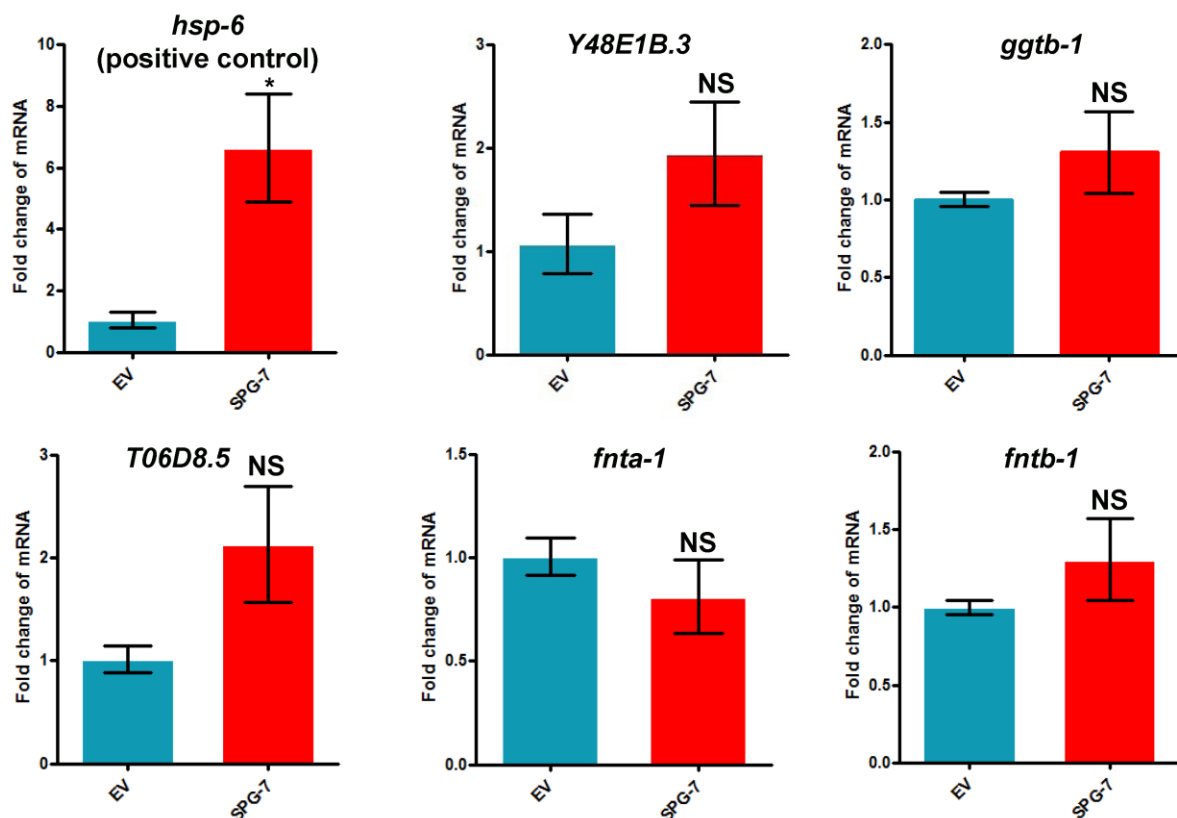


**Figure S16. qPCR data of the *hsp-6* positive control gene and genes unmodified significantly by the UPR<sup>mt</sup>**

The expression level of *hsp-6* was used as a positive control for the UPR<sup>mt</sup> response. No significant change was detected for Y48E1B.3, *ggtb-1*, T06D8.5, *fnta-1*, and the *fntb-1* genes. Error bars represent standard errors of the mean. “NS” indicates no significant difference in the relative expression level. “\*” $p \leq 0.05$ ; “\*\*” $p \leq 0.01$ ; “\*\*\*” $p \leq 0.001$  using two-tailed, unpaired Student’s T-tests.

***coq-1<sub>pr</sub>::coq-1::gfp***

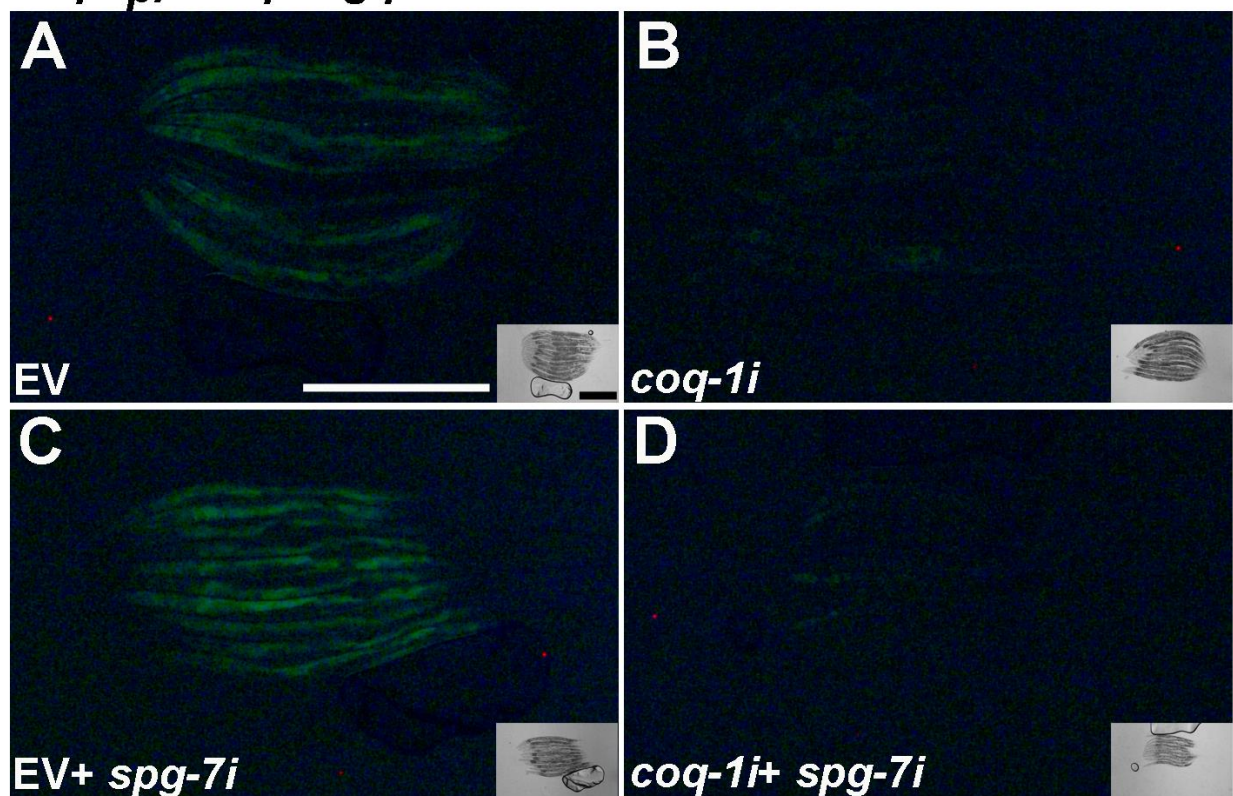


**Figure S17. *coq-1* RNAi abolishes the COQ-1::GFP signal**

A) Worms expressing the *coq-1<sub>pr</sub>::coq-1::gfp* transgene (hereafter COQ-1::GFP) treated with empty vector control bacteria. B) *coq-1* RNAi reduces the level of the COQ-1::GFP signal. C) *spg-7* RNAi induces the upregulation of the COQ-1::GFP protein even when diluted by half with an empty vector control. D) *coq-1* RNAi abolishes the COQ-1::GFP signal upon treatment with *spg-7* RNAi. These results show that the *gfp* signal of the

COQ-1::GFP construct and the *coq-1* RNAi are both corresponding to the *coq-1* gene. Scale bars represent 500µM.

## **Supplemental methods**

### **Biochemical assay for the activity of HMGCR proteins**

#### **Protein expression and purification**

The HMSG-1/HMGCS1 assay was based on a well-established published data about a method to measure the enzymatic activity of HMGCS1 *in vitro* (SKAFF AND MIZIORKO 2010). In brief, the *C. elegans hmgs-1* and Human *hmgcs1* genes were cloned in pET28b plasmids. This cloning resulted in proteins that were tagged at their N-terminus by 6X histidine tags. After validating by sequencing that the plasmids harbor intact proteins, plasmids were transformed into BL21 (DE3) bacteria that were then plated on Kanamycin (50µg/ml) plates and grown in an 37°C incubator overnight. The next day, slurs of colonies were grown for eight hours in 100ml LB at 37°C in the presence of Kanamycin (50µg/ml). Next, these bacterial cultures were pre-incubated for 30 minutes in an 20°C incubator before 1mM IPTG (Sigma) was added, and the cultures were incubated overnight at 20°C. Cultures were harvested at 4000 rpm for 30 minutes, and bacterial pellets were resuspended in 6ml of lysis buffer (100mM NaCl, 50mM Tris pH. 8, 5mM Imidazole, and 1mM PMSF) prior to transfer into 15ml tubes. Bacteria were lysed by 12 cycles of ten seconds sonication followed by ten seconds recovery (total two minutes of sonication per sample). Next, lysates were spun 30 minutes at 14,000 rpm at 4°C and the upper phase was transferred to a new tube. 100µl of NiNTA beads (Thermo Fisher Scientific), pre-washed three times with the lysis buffer, were added to each tube, and the tubes were incubated for 3.5 hours at 4°C. Next, tubes were spun at 1700 rpm for one minute and fresh 5ml of lysis buffer was added to each pellet. This step was repeated three more times. At the last washing step, the lysates with the beads were transferred to Eppendorf tubes, spun once more, and the upper phase was aspirated. Next, the proteins bound to the pellet of beads were eluted by adding 400µl of lysis buffer with 500mM Imidazole. Tubes were incubated with agitation at 4°C for 30 minutes followed by spinning, at 1700 rpm, for one minute before the upper phases were collected. From each eluate, 2.5µl was ran on a protein gel to examine the

specificity of the purification. In parallel, protein concentration was determined using the Bradford method (BioRad). The sizes of the purified proteins were in agreement with their predicted molecular weights (51.4 kDa for HMGS-1 and 57.2 kDa for HMGCS1). To wash the imidazole away, samples were loaded on Amicon Ultra-0.5mL Centrifugal Filters (pore size 10kDa) and washed five times with 300µl phosphate buffer (10mM KPO<sub>4</sub> pH.7) before samples were eluted in 100µl of the same buffer. The Centrifugal Filters were spun at 3000 rpm for one minute each time. Samples were kept on ice up to one day for the assay or mixed with glycerol (final concentration 15% of glycerol) and were frozen in -80°C for future use.

### **Assay for the activity of HMGCS *in vitro***

The assay was conducted in triplicates. For each reaction, 1µg of protein was used in a final volume of 120µl solution containing 70µM TRIS-HCl pH 8.0, 130µM DTNB (Sigma D8130-500MG), 65 µM Acetyl-CoA sodium salt (Sigma A2056-1MG), 10 µM Acetoacetyl-CoA sodium salt (MP 150224). After setting the reactions up in a 96 well plate, the plate was placed in a Synergy HTX Plate Reader (BioTek) for a time-course analysis at 25°C. The level of fluorescent signal, at 412nm, was determined every 30 seconds for a total time of ten minutes. Enzyme activities in the linear region of the graphs (between 00:30 and 03:30) are 0.466 units +/-0.25 for HMGS-1 and 0.488 units +/-0.054 for HMGCS1. Definition of a unit= 1µM of the substrate converted to the product per minute per 1µg of the purified enzyme.

### **References**

- Gallegos, M. E., S. Balakrishnan, P. Chandramouli, S. Arora, A. Azameera *et al.*, 2012 The C. elegans rab family: identification, classification and toolkit construction. PLoS One 7: e49387.
- Skaff, D. A., and H. M. Miziorko, 2010 A visible wavelength spectrophotometric assay suitable for high-throughput screening of 3-hydroxy-3-methylglutaryl-CoA synthase. Anal Biochem 396: 96-102.